Available online at www.sciencedirect.com
ScienceDirect
Carbohydrate Research 342 (2007) 2735–2744
Carbohydrate RESEARCH

Structural determination of a neutral exopolysaccharide produced by *Lactobacillus delbrueckii* ssp. *bulgaricus* LBB.B332

Inmaculada Sánchez-Medina,[a] Gerrit J. Gerwig,[a] Zoltan L. Urshev[b] and Johannis P. Kamerling[a,*]

[a]*Bijvoet Center, Department of Bio-Organic Chemistry, Utrecht University, Padualaan 8, NL-3584 CH Utrecht, The Netherlands*
[b]*LB Bulgaricum Plc., R&D Center, 12A Malashevska Str., Sofia 1202, Bulgaria*

Received 15 August 2007; accepted 14 September 2007
Available online 22 September 2007

Abstract—The neutral exopolysaccharide produced by *Lactobacillus delbrueckii* ssp. *bulgaricus* LBB.B332 in skimmed milk was found to be composed of D-glucose, D-galactose, and L-rhamnose in a molar ratio of 1:2:2. Linkage analysis and 1D/2D NMR (^{1}H and ^{13}C) studies carried out on the native polysaccharide as well as on an oligosaccharide generated by a periodate oxidation protocol, showed the polysaccharide to consist of linear pentasaccharide repeating units with the following structure:

→3)-α-D-Glc*p*-(1→3)-α-D-Gal*p*-(1→3)-α-L-Rha*p*-(1→2)-α-L-Rha*p*-(1→2)-α-D-Gal*p*-(1→

Keywords: *Lactobacillus delbrueckii* ssp. *bulgaricus*; Exopolysaccharide; Lactic acid bacteria; Structural analysis; NMR spectroscopy; Mass spectrometry

1. Introduction

Microbial exopolysaccharides (EPSs) produced by lactic acid bacteria are of increasing interest to the food industry. Their particular physical and rheological properties, which make them suitable as viscosifying, stabilizing, gelling, or emulsifying agents,[1] in combination with the GRAS (generally recognized as safe) status of EPS-producing lactic acid bacteria, make EPSs promising as a new generation of food thickeners. To unravel the relationship between their structure and physical properties, structural studies have been performed on EPSs produced by different species of lactic acid bacteria, such as *Lactobacillus*, *Lactococcus*, and *Streptococcus* genera.[2]

Lactobacillus delbrueckii ssp. *bulgaricus* strains are used in combination with *Streptococcus thermophilus* strains as commercial yoghurt starters. Several EPSs produced by *Lb. delbrueckii* ssp. *bulgaricus* have been characterized, being mainly composed of Glc and Gal[3–6] or of Glc, Gal, and Rha.[7–10]

Here, we report on the structure of the neutral EPS produced by *Lb. delbrueckii* ssp. *bulgaricus* LBB.B332 in skimmed milk.

2. Results and discussion

2.1. Isolation, purification and composition of the exopolysaccharide

The neutral EPS produced by *Lb. delbrueckii* ssp. *bulgaricus* LBB.B332 was isolated via absolute ethanol precipitation of the trichloroacetic acid-treated culture medium, and further purified by anion-exchange chromatography on DEAE-Trisacryl Plus M. Its average

* Corresponding author. Tel.: +31 30 253 34 79; fax: +31 30 254 09 80; e-mail: j.p.kamerling@uu.nl

0008-6215/$ - see front matter © 2007 Elsevier Ltd. All rights reserved.
doi:10.1016/j.carres.2007.09.005

Table 1. Methylation analysis data of *Lactobacillus delbrueckii* ssp. *bulgaricus* LBB.B332 neutral EPS and oligosaccharide TRI

Partially methylated alditol acetate	t_R[a]	Structural feature	Molar ratio EPS[b]	Molar ratio TRI[b]
3,4-Di-*O*-methyl-1,2,5-tri-*O*-acetylrhamnitol-*1-d*	0.92	→2)-Rha*p*-(1→	1.00	—
2,4-Di-*O*-methyl-1,3,5-tri-*O*-acetylrhamnitol-*1-d*	0.94	→3)-Rha*p*-(1→	0.83	0.7
2,3,4,6-Tetra-*O*-methyl-1,5-di-*O*-acetylglucitol-*1-d*	1.00	Glc*p*-(1→	—	1.0
2,4,6-Tri-*O*-methyl-1,3,5-tri-*O*-acetylglucitol-*1-d*	1.18	→3)-Glc*p*-(1→	0.81	—
2,4,6-Tri-*O*-methyl-1,3,5-tri-*O*-acetylgalactitol-*1-d*	1.23	→3)-Gal*p*-(1→	1.83	1.1
3,4,6-Tri-*O*-methyl-1,2,5-tri-*O*-acetylgalactitol-*1-d*		→2)-Gal*p*-(1→		—

[a] GLC retention times relative to 2,3,4,6-tetra-*O*-methyl-1,5-di-*O*-acetylglucitol-*1-d* on EC-1.
[b] Calculated from peak areas, not corrected by response factors.

molecular mass of 1.3×10^6 Da was determined by gel-filtration chromatography on Sephacryl S-400 HR.

Quantitative monosaccharide analysis, including absolute configuration determination, of the EPS gave D-Glc, D-Gal, and L-Rha in a molar ratio of 1.0:2.0:2.1. Methylation analysis (Table 1) showed the presence of 3-substituted Glc*p*, 3-substituted Gal*p*, 2-substituted Gal*p* (coeluting with the 3-substituted Gal*p* in the gas chromatogram), 2-substituted Rha*p*, and 3-substituted Rha*p*, in a molar ratio of 0.8:1.8:1.0:0.8, suggesting a repeating linear pentasaccharide with all residues in the pyranose ring form.

The 1D ^{1}H NMR spectrum of the EPS (Fig. 1) showed five signals of equal intensity in the anomeric region (δ 5.0–5.5), supporting a pentasaccharide repeating unit. The constituting monosaccharide units in the EPS were arbitrarily named from **A** to **E**, according to the decreasing chemical shift values of their anomeric protons. Their δ values suggest the occurrence of α-configurations only. The spectrum presents one high-field signal at δ 1.307, arising from the methyl groups of two Rha residues.

2.2. Periodate oxidation and analysis of the trisaccharide TRI

The material obtained after periodate oxidation[11] of the EPS and subsequent dialysis was subjected to monosaccharide analysis, showing D-Glc, D-Gal, and L-Rha in a molar ratio of 1.0:1.0:1.1, which indicated the loss of one Gal and one Rha residue with respect to the native EPS. After reduction with $NaBH_4$ and dialysis of the sample, monosaccharide analysis confirmed the presence of equimolar amounts of D-Glc, D-Gal, and L-Rha. The degraded, but still polymeric material was subjected to mild acid hydrolysis (0.5 M TFA, 80 °C), showing after 30 min a major TLC band in the trisaccharide region; fractionation on Bio-Gel P-2 yielded a main fraction,

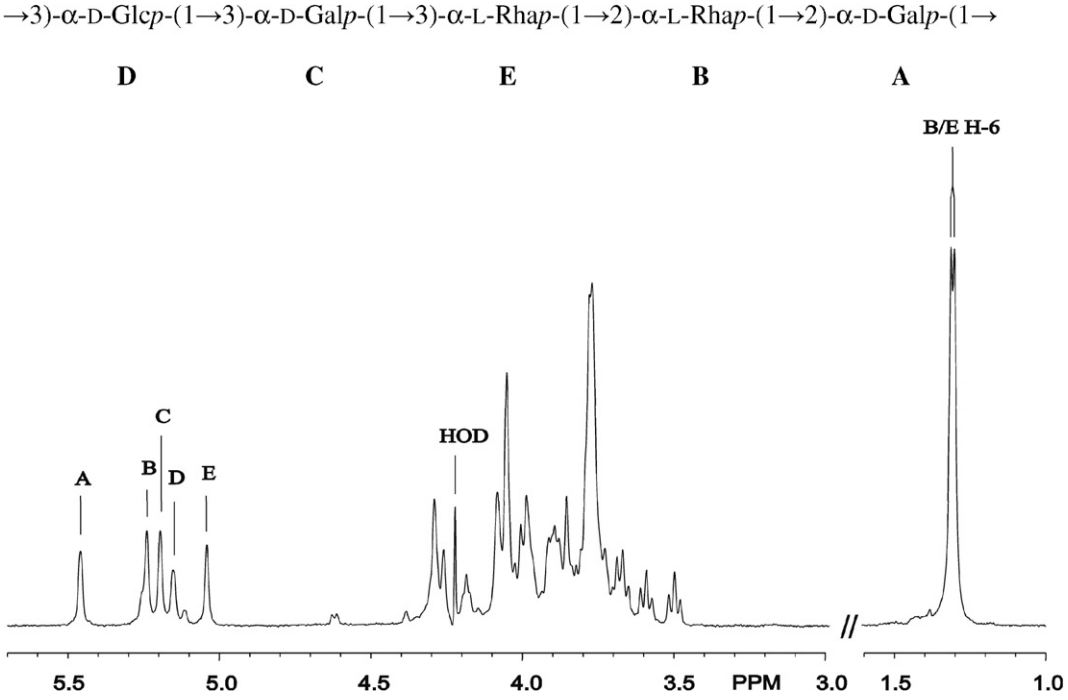

Figure 1. 500-MHz 1D ^{1}H NMR spectrum of the neutral EPS produced by *Lactobacillus delbrueckii* ssp. *bulgaricus* LBB.B332, recorded in D_2O at 78 °C.

denoted TRI. MALDI-TOF-MS of TRI showed a $[M+Na]^+$ pseudomolecular ion at m/z 510.67, together with a $[M+K]^+$ ion at m/z 527.16, corresponding with Hex_2dHex ($M = 488.17$ Da). According to the periodate oxidation protocol, after mild acid hydrolysis an additional glyceraldehyde group should be attached to the reducing end. The absence of this group, as indicated by MALDI-TOF-MS, is caused by the acid lability of the rhamnosyl glyceraldehyde linkage under acidic conditions. A similar situation had been previously reported.[12]

Monosaccharide analysis of TRI demonstrated Hex_2dHex to be built up from D-Glc, D-Gal, and L-Rha. Linkage analysis (Table 1) showed the presence of terminal Glc*p*, 3-substituted Gal*p*, and 3-substituted Rha*p*, in a molar ratio of 1.0:1.1:0.7, in accordance with a linear trisaccharide structure.

MALDI-TOF-MS analysis of $NaBH_4$-reduced TRI showed $[M+Na]^+$ and $[M+K]^+$ pseudomolecular ions at m/z 513.33 and 529.03, respectively, corresponding with Hex_2dHex-ol ($M = 490.19$ Da). Monosaccharide analysis revealed Glc, Gal, and Rha-ol in a molar ratio of 0.9:1.0:1.0, whereas methylation analysis, following a methanolysis/trimethylsilylation protocol, indicated the presence of terminal Glc*p*, 3-substituted Gal*p*, and 3-substituted Rha-ol in a molar ratio of 1.0:1.3:0.6. 1D ^{1}H NMR analysis showed two anomeric signals, that is, terminal Glc **D** H-1 at δ 5.120 ($^3J_{1,2}$ 3.9 Hz) and Gal **C** H-1 at δ 5.264 ($^3J_{1,2}$ 3.5 Hz). The combined results establish the following structure for the trisaccharide-alditol:

α-D-Glc*p*-(1→3)-α-D-Gal*p*-(1→3)-L-Rha-ol

D **C** **E**

In order to generate supporting NMR data on the trisaccharide level for the NMR analysis of the EPS, TRI was investigated in great detail. The 1D ^{1}H NMR spectrum of TRI (Fig. 2) showed four major signals in the anomeric proton region at δ 5.188 (residue $\mathbf{C}_\beta$, $^3J_{1,2}$ 3.9 Hz), δ 5.162 (residue $\mathbf{C}_\alpha$, $^3J_{1,2}$ 3.9 Hz; residue **E**α, $^3J_{1,2}$ <1 Hz), δ 5.141 (residue **D**, $^3J_{1,2}$ 3.9 Hz), and δ 4.877 (residue **E**β, $^3J_{1,2}$ <1 Hz). Taking into account the δ values of residues **D** and **C**, combined with the methylation analysis data, the α-pyranose configuration is assigned for both units. Residue **E** corresponds to the reducing Rha unit. Splitting of **C** into $\mathbf{C}_\alpha$ and $\mathbf{C}_\beta$ is observed as a consequence of the linkage between **C** and **E**.

The ^{1}H chemical shifts of all protons of TRI (Table 2) were obtained by means of 2D TOCSY (mixing times, 40–100 ms), ROESY (mixing time, 300 ms), and ^{1}H–^{13}C HSQC experiments. The TOCSY spectrum of TRI with a mixing time of 100 ms is shown in Figure 3, together with the ROESY spectrum. The ^{1}H–^{13}C HSQC spectrum is shown in Figure 4. Starting points for the interpretation of the spectra were the anomeric

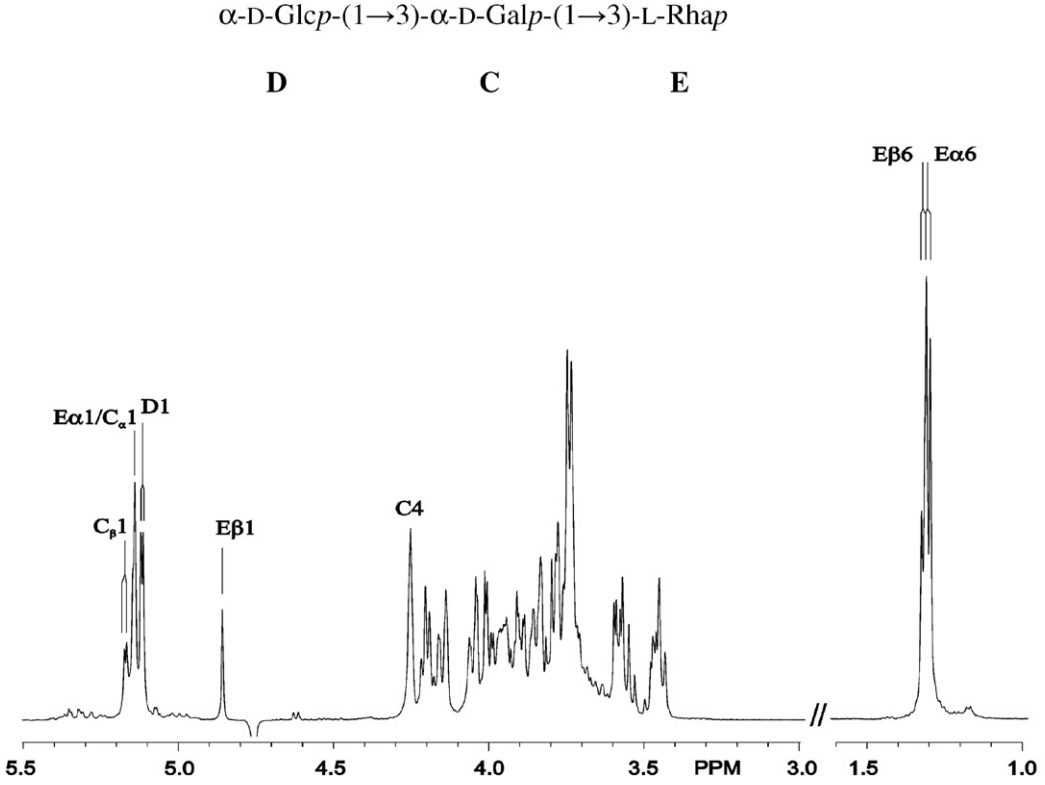

Figure 2. 500-MHz 1D ^{1}H NMR spectrum of oligosaccharide TRI, recorded in D_2O at 27 °C.

Table 2. ^{1}H and ^{13}C NMR chemical shifts[a] of EPS, recorded in D_2O at 78 °C, and oligosaccharide TRI, recorded in D_2O at 27 °C

Residue	Proton	EPS	TRI	Carbon	EPS	TRI
→2)-α-D-Gal*p*-(1→ **A**	H-1	5.458	—	C-1	99.4 (179)	—
	H-2	3.98	—	C-2	75.6	—
	H-3	4.05	—	C-3	70.5	—
	H-4	4.07	—	C-4	71.1	—
	H-5	4.30	—	C-5	72.1	—
	H-6a	3.78	—	C-6	62.3	—
	H-6b	3.78	—			
→2)-α-L-Rha*p*-(1→ **B**	H-1	5.239	—	C-1	101.5 (172)	—
	H-2	4.09	—	C-2	79.5	—
	H-3	3.92	—	C-3	71.4	—
	H-4	3.51	—	C-4	73.6	—
	H-5	3.84	—	C-5	70.5	—
	CH_3	1.307	—	CH_3	17.7	—
→3)-α-D-Gal*p*-(1→ **C**	H-1	5.196	5.162/5.188 (3.9)	C-1	96.8 (172)	100.2/100.0 (171)
	H-2	4.05	4.06/4.01	C-2	68.1	71.4
	H-3	4.06	4.01/4.06	C-3	76.2	79.4
	H-4	4.27	4.26	C-4	67.1	70.3
	H-5	4.19	4.21	C-5	71.9	75.2
	H-6a	3.77	3.75	C-6	62.3	65.4
	H-6b	3.77	3.75			
→3)-α-D-Glc*p*-(1→ **D**	H-1	5.154	—	C-1	96.7 (174)	—
	H-2	3.74	—	C-2	71.4	—
	H-3	4.00	—	C-3	80.3	—
	H-4	3.68	—	C-4	71.5	—
	H-5	4.00	—	C-5	73.2	—
	H-6a	3.86	—	C-6	61.9	—
	H-6b	3.79	—			
→3)-α-L-Rha*p*-(1→ **E**	H-1	5.042	—	C-1	103.1 (170)	—
	H-2	4.29	—	C-2	68.1	—
	H-3	3.90	—	C-3	76.8	—
	H-4	3.59	—	C-4	71.8	—
	H-5	3.77	—	C-5	70.5	—
	CH_3	1.307	—	CH_3	17.7	—
α-D-Glc*p*-(1→ **D**	H-1	—	5.141 (3.9)	C-1	—	100.2 (171)
	H-2	—	3.59	C-2	—	76.2
	H-3	—	3.80	C-3	—	77.6
	H-4	—	3.46	C-4	—	74.2
	H-5	—	3.96	C-5	—	76.6
	H-6a	—	3.85	C-6	—	65.0
	H-6b	—	3.78			
→3)-α-L-Rha*p* **Eα**	H-1	—	5.162 (<1)	C-1	—	98.5 (170)
	H-2	—	4.15	C-2	—	72.0
	H-3	—	3.90	C-3	—	79.8
	H-4	—	3.56	C-4	—	75.2
	H-5	—	3.93	C-5	—	73.1
	CH_3	—	1.299	CH_3	—	17.1
→3)-β-L-Rha*p* **Eβ**	H-1	—	4.877 (<1)	C-1	—	98.3 (n.d.)
	H-2	—	4.17	C-2	—	72.2
	H-3	—	3.72	C-3	—	82.0
	H-4	—	3.48	C-4	—	74.8
	H-5	—	3.46	C-5	—	76.7
	CH_3	—	1.322	CH_3	—	17.1

$^{3}J_{1,2}$ and $^{1}J_{C\text{-}1,H\text{-}1}$ coupling constants are included in parentheses.

[a] In ppm relative to the signal of internal acetone at δ 2.225 for ^{1}H, and in ppm relative to the signal of external [1-^{13}C] glucose ($\delta_{C\text{-}1}$ 92.9) for ^{13}C.

signals of residues $\mathbf{C}_\alpha$, $\mathbf{C}_\beta$, **D**, **E**α, and **E**β, and the methyl signals of rhamnose residues **E**α and **E**β. Comparison of TOCSY spectra with increasing mixing times allowed the assignment of the sequential order of the chemical shifts belonging to the same spin system.

The characteristic spin system seen on the TOCSY H-1 track of residue **D** (H-2,3,4,5,6a,6b) indicated a *gluco*-

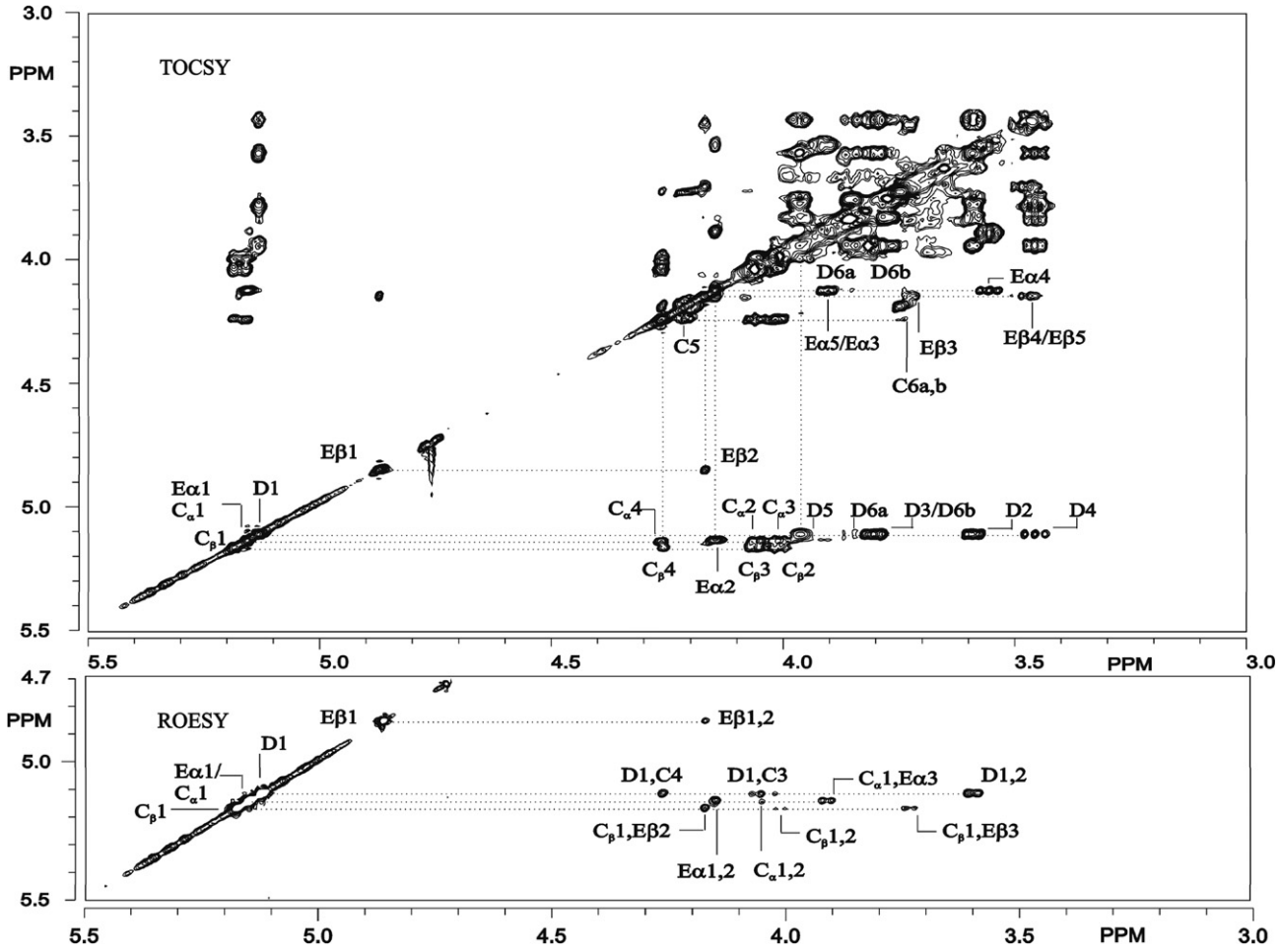

Figure 3. 2D TOCSY (mixing time, 100 ms) and ROESY (mixing time, 300 ms) spectra of the oligosaccharide TRI, recorded in D_2O at 27 °C. The CH_3 signals were observed at 1.30 and 1.32 ppm, but were not included in the picture. Cross-peaks belonging to the same scalar-coupling network are indicated near a dotted line starting from the corresponding diagonal peaks; TOCSY: D1 corresponds to the diagonal peak of residue **D** H-1; D2 refers to a cross-peak between **D** H-1 and **D** H-2, etc.; ROESY: D1 corresponds to the diagonal peak of residue **D** H-1; D1,2 refers to an intra-residue cross-peak between **D** H-1 and **D** H-2, and D1,C4 indicates an inter-residue connectivity between **D** H-1 and **C** H-4, etc.

configuration, whereas those found on the TOCSY H-1 tracks of residues $\mathbf{C}_\alpha$ and $\mathbf{C}_\beta$ (H-2,3,4) a *galacto*-configuration. Note the typical upfield positions of Glc H-2 and H-4, and the typical downfield position of Gal H-4. The finding of only one cross-peak (H-2) on the TOCSY H-1 tracks of both residues **E**α and **E**β is in agreement with a *rhamno*-configuration. In both cases a correlation with the related upfield CH_3 signal is detected.

The ^{13}C resonances of TRI (Table 2) were determined by interpretation of the ^{1}H–^{13}C HSQC spectrum (Fig. 4), whereas a 2D ^{1}H–^{13}C HMBC spectrum revealed the $^{1}J_{C\text{-}1,H\text{-}1}$ coupling constants. The $^{1}J_{C\text{-}1,H\text{-}1}$ values of 171 Hz for Gal*p* **C** and Glc*p* **D** confirmed their α configuration.[13]

By comparison of the ^{13}C chemical shifts of residues $\mathbf{C}_\alpha$, $\mathbf{C}_\beta$, **D**, **E**α, and **E**β with those of (methyl) aldosides,[14] going for typical downfield shifts, the occurrence of a terminal α-Glc*p* **D** unit (compare with α-D-Glc*p*1Me), a 3-substituted α-Gal*p* **C** unit (**C** C-3, δ 79.4; α-D-Gal*p*1Me, $\delta_{C\text{-}3}$ 70.5), and a 3-substituted α-Rha*p* **E** unit (**E**α C-3, δ 79.8; α-L-Rha*p*, $\delta_{C\text{-}3}$ 71.1; **E**β C-3, δ 82.0; β-L-Rha*p*, $\delta_{C\text{-}3}$ 73.8) could be verified.[14]

Finally, sequence analysis data followed from inter-residue ROESY cross-peaks (Fig. 3) and ^{1}H–^{13}C HMBC long-range couplings. The **D**(1→3)**C** linkage is reflected by the ROESY cross-peaks **D** H-1/**C** H-3,4 and the ^{1}H–^{13}C HMBC connectivity observed between **D** C-1 and **C**β H-3. The **C**(1→3)**E** linkage fits the ROESY cross-peaks $\mathbf{C}_\alpha$ H-1/**E**α H-2,3 and $\mathbf{C}_\beta$ H-1/**E**β H-2,3. A ^{1}H–^{13}C HMBC connectivity between **C**α C-1 and **E**α H-3 confirms this linkage.

Taking together all information obtained, the structure of TRI can be formulated as

α-D-Glc*p*-(1→3)-α-D-Gal*p*-(1→3)-L-Rha*p*

D **C** **E**

2.3. 2D NMR spectroscopy of the native polysaccharide

The complete assignment of the ^{1}H and ^{13}C chemical shifts of the native EPS (Table 2) was made by means of 2D TOCSY (mixing times, 40–100 ms), NOESY (mixing time, 150 ms), and ^{1}H–^{13}C HSQC experiments. The TOCSY spectrum (100 ms) of the EPS is shown in Figure 5, together with the NOESY spectrum. The ^{1}H–^{13}C HSQC spectrum is shown in Figure 6. Starting points for the interpretation of the spectra were the anomeric signals of the residues **A**–**E**, and the methyl signals of the Rha residues **B** and **E**. Comparison of TOCSY spectra with increasing mixing times allowed the assignment of the sequential order of the chemical shifts belonging to the same spin system.

The TOCSY **A** H-1 track (δ 5.458) showed cross-peaks with **A** H-2,3,4. The resonances for **A** H-5,6a,6b were found in the HSQC spectrum. Using the TOCSY **B** H-2 track, found via the **B** H-1 track (δ 5.239), the resonances for **B** H-3,4,5,CH_3 were detected. The TOCSY **C** H-1 track (δ 5.196) revealed the cross-peaks with **C** H-2,3,4,5, whereas on the **C** H-5 track the cross-peak with **C** H-6a,b was found. The TOCSY **D** H-1 track (δ 5.154) showed cross-peaks with **D** H-2,3,4. The assignment of the **D** H-5,6a,6b resonances was made via the ^{1}H–^{13}C HSQC spectrum. Finally, via the TOCSY **E** H-1 track (δ 5.042) the **E** H-2 track was found, which showed the cross-peaks with **E** H-3,4,5,CH_3.

As is evident from the TOCSY results, residues **B** and **E**, with the short H-1 tracks (only H-2 is seen) and the typical H-6 signals for 6-deoxyhexoses, represent the Rha residues. The TOCSY results for residue **D** indicate a *gluco*-configuration, whereas the spin systems of residues **A** and **C**, with downfield positions of H-4, are in agreement with a *galacto*-configuration.

Evaluation of the C-1 chemical shifts (Table 2; Fig. 6) and the $^{1}J_{C\text{-}1,H\text{-}1}$ coupling constants, deduced from 2D ^{1}H–^{13}C HMBC experiments, confirmed that all residues occur in α-pyranosyl form:[13] residue **A**/Gal, δ 99.4, $^{1}J_{C\text{-}1,H\text{-}1}$ 179 Hz; residue **B**/Rha, δ 101.5, $^{1}J_{C\text{-}1,H\text{-}1}$ 172 Hz; residue **C**/Gal, δ 96.8, $^{1}J_{C\text{-}1,H\text{-}1}$ 172 Hz; residue **D**/Glc, δ 96.8, $^{1}J_{C\text{-}1,H\text{-}1}$ 174 Hz; and residue **E**/Rha, δ 103.1, $^{1}J_{C\text{-}1,H\text{-}1}$ 170 Hz. The relatively high $^{1}J_{C\text{-}1,H\text{-}1}$ value of residue **A** had been reported previously for 2-substituted monosaccharides,[12,15,16] and is probably due to the 2-substitution. Note that the α-anomeric configuration of the two Rha residues follows also from a comparison of the chemical shifts of their H-5 atoms (**B** H-5, δ 3.84; **E** H-5, δ 3.77) with those of α-L-Rha*p*1Me (H-5, δ 3.66) and β-L-Rha*p*1Me (H-5, δ 3.39).[17]

Taking into account the published ^{13}C chemical shift data of methyl aldosides,[14] and the methylation analysis data of the EPS (Table 1), residue **A** was assigned as 2-substituted α-Gal*p* (downfield shift of **A** C-2, δ 75.6; α-D-Gal*p*1Me, $\delta_{C\text{-}2}$ 69.2), residue **B** as 2-substituted α-Rha*p* (downfield shift of **B** C-2, δ 79.5; α-L-Rha*p*1Me, $\delta_{C\text{-}2}$ 71.0), residue **C** as 3-substituted α-Gal*p* (downfield shift of **C** C-3, δ 76.2; α-D-Gal*p*1Me, $\delta_{C\text{-}3}$ 70.5), residue **D** as 3-substituted α-Glc*p* (downfield shift of **D** C-3, δ 80.3; α-D-Glc*p*1Me, $\delta_{C\text{-}3}$ 74.1), and residue **E** as 3-substituted α-Rha*p* (downfield shift of **E** C-3, δ 76.8; α-L-Rha*p*1Me, $\delta_{C\text{-}3}$ 71.3).

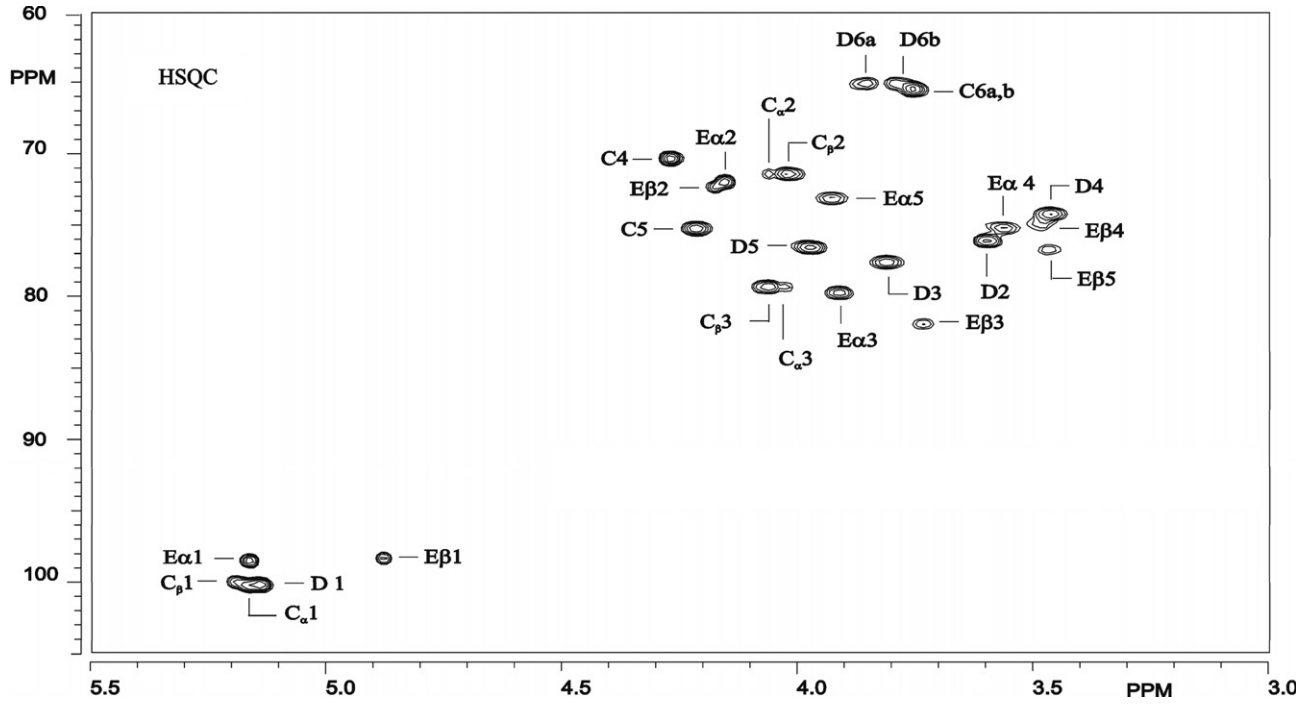

Figure 4. 2D ^{1}H–^{13}C HSQC spectrum of the oligosaccharide TRI, recorded in D_2O at 27 °C. The CH_3 signals were observed at 1.30/17.1 and 1.32/17.1 ppm, but were not included in the picture. D1 corresponds to the cross-peak between **D** H-1 and **D** C-1, etc.

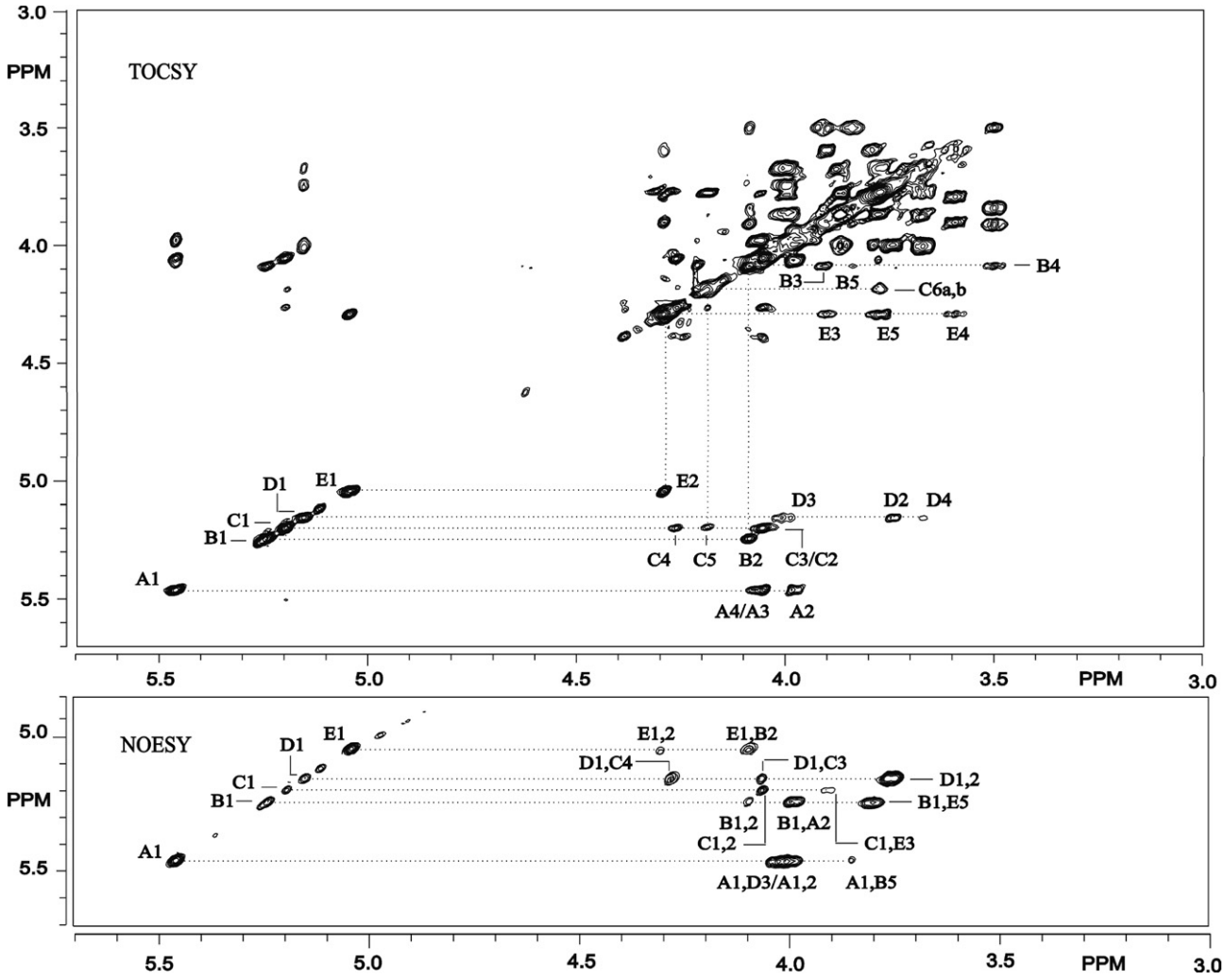

Figure 5. 2D TOCSY (mixing time, 100 ms), and NOESY (mixing time, 150 ms) spectra of EPS, recorded in D_2O at 78 °C. The CH_3 signals were observed at 1.31 ppm, but were not included in the picture. Cross-peaks belonging to the same scalar-coupling network are indicated near a dotted line starting from the corresponding diagonal peaks; TOCSY: D1 corresponds to the diagonal peak of residue **D** H-1; D2 refers to a cross-peak between **D** H-1 and **D** H-2, etc.; NOESY: D1 corresponds to the diagonal peak of residue **D** H-1; D1,2 refers to an intra-residue cross-peak between **D** H-1 and **D** H-2, and D1,C4 indicates an inter-residue connectivity between **D** H-1 and **C** H-4, etc.

The establishment of the sequence of the monosaccharide residues within the repeating unit of the EPS was made by the assignment of the inter-residue cross-peaks in the 2D NOESY spectrum (Fig. 5) and the relevant long-range couplings in the HMBC spectrum (Table 3). Inspection of the NOESY spectrum showed on the **E** H-1 track an inter-residue cross-peak with **B** H-2, indicating a **E**(1→2)**B** linkage. On the **B** H-1 NOESY track, a connectivity was found between **B** H-1 and **A** H-2, leading to the assignment of a **B**(1→2)**A** linkage. The inter-residue **A** H-1,**D** H-3 connectivity supports the occurrence of an **A**(1→3)**D** linkage. The observed NOESY cross-peaks between **D** H-1 and **C** H-3,4, combined with the methylation analysis/^{13}C NMR data for residue **C** (vide supra) demonstrated a **D**(1→3)**C** linkage. Finally, the inter-residue connectivity **C** H-1/**E** H-3 allowed the assignment of the **C**(1→3)**E** linkage. The observed intra-residue NOE connectivities were in accordance with the assigned anomeric configurations. Interestingly, two more inter-residue cross-peaks were detected in the NOESY spectrum, namely, **A** H-1/**B** H-5 and **B** H-1/**E** H-5, of importance for future conformational studies of the EPS.

Combining the various data of the EPS analysis, supported by the structural determination of the generated trisaccharide fragment, demonstrates the polysaccharide to be built up from the following pentasaccharide repeating unit:

→3)-α-D-Glc*p*-(1→3)-α-D-Gal*p*-(1→3)-α-L-Rha*p*-(1→2)-α-L-Rha*p*-(1→2)-α-D-Gal*p*-(1→

D **C** **E** **B** **A**

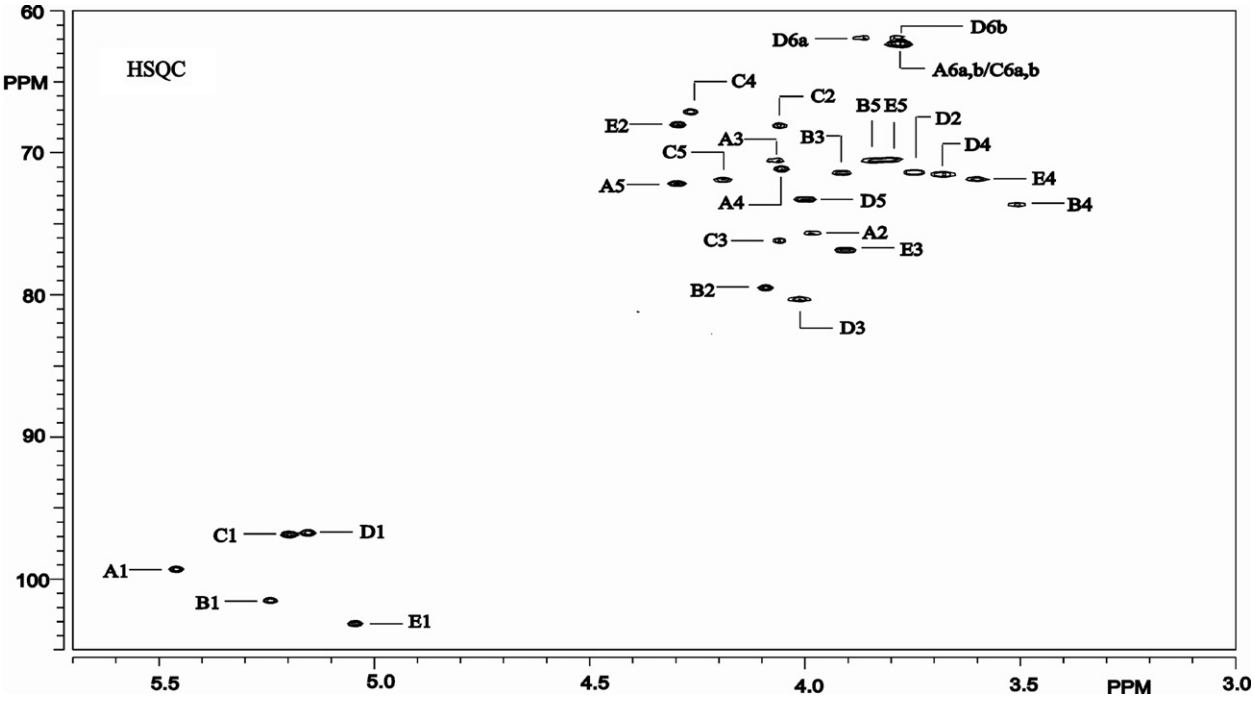

Figure 6. 2D ^{1}H–^{13}C HSQC spectrum of EPS, recorded in D_2O at 78 °C. The CH_3 signals were observed at 1.31/17.7 ppm, but were not included in the picture. D1 corresponds to the cross-peak between **D** H-1 and **D** C-1, etc.

Table 3. Long-range ^{1}H–^{13}C couplings found in the HMBC spectrum for the anomeric signals of the residues of the EPS

Residue	$\delta_{H\text{-}1/C\text{-}1}$	Connectivities	Residue
A	5.458	80.3	**D** C-3
		72.1	**A** C-5
		70.5	**A** C-3
	99.4	4.00	**D** H-3
B	5.239	79.5	**B** C-2
		75.6	**A** C-2
		71.4	**B** C-3
		70.5	**B** C-5
	101.5	3.98	**A** H-2
C	5.196	76.8	**E** C-3
		76.2	**C** C-3
		71.9	**C** C-5
	96.8	3.90	**E** H-3
D	5.154	80.3	**D** C-3
		76.2	**C** C-3
		73.2	**D** C-5
E	5.042	79.5	**B** C-2
		76.8	**E** C-3
		70.5	**E** C-5
		68.1	**E** C-2
	103.1	4.29	**E** H-2
		4.09	**B** H-2

A: →2)-α-D-Gal*p*-(1→; **B**: →2)-α-L-Rha*p*-(1→; **C**: →3)-α-D-Gal*p*-(1→; **D**: →3)-α-D-Glc*p*-(1→; **E**: →3)-α-L-Rha*p*-(1→.

2.4. Final remarks

The structure established for the EPS of *Lb. delbrueckii* ssp. *bulgaricus* LBB.B332 shows some similarities with other branched EPSs produced by *S. thermophilus*[12,15,18–20] and *Lactococcus lactis* ssp. *cremoris*[16] strains. All these EPSs have the same pentameric backbone consisting of a →3)-α-D-Gal*p*-(1→3)-α-L-Rha*p*-(1→2)-α-L-Rha*p*-(1→2)-α-D-Gal*p*-(1→3)-Hex*p*-(1→ sequence, differing in the fifth residue: an α-D-Glc*p* unit in the case of *Lactococcus lactis* ssp. *cremoris* B39,[16] *S. thermophilus* Sfi12,[19] and *Lb. delbrueckii* ssp. *bulgaricus* LBB.B332; an α-D-Gal*p* unit in the case of *S. thermophilus* Rs,[15] Sts,[15] OR 901[18] (three identical repeating units), and MR-1C;[20] or a β-D-Gal*p* unit in the case of *S. thermophilus* S3.[12] Furthermore, they also keep the fourth position of the 3-substituted α-L-Rha*p* unit as the branching point, with the exception of the EPS of *S. thermophilus* S3, which has it at the sixth position of the 3-substituted α-D-Gal*p*. However, more variations are found in the structure of the side chains. They can vary from single β-D-Gal*p*[19] or β-D-Gal*f*[12] units to disaccharides such as β-D-Gal*p*-(1→4)-β-D-Glc*p*[16] or β-D-Gal*p*-(1→6)-β-D-Gal*p*.[15,18] The latter is also found in the EPS of *S. thermophilus* MR-1C, together with a second side chain, consisting of a L-Fuc unit.[20] This could mean that these bacteria have a very similar pathway for the biosynthesis of their corresponding EPSs.

3. Experimental

3.1. Production, isolation, and purification of the exopolysaccharide

The *Lb. delbrueckii* ssp. *bulgaricus* LBB.B332 strain, isolated from home-made yoghurt, was obtained from the

LBB collection of LB Bulgaricum Plc. (Sofia, Bulgaria). An aliquot of an activated bacterial culture was used to inoculate 1 L of sterile (121 °C, 7 min) reconstituted skimmed milk powder in water (10% w/v; E. Merck, Darmstadt, Germany), and the strain was grown for 24 h at 42 °C. After incubation, proteins were removed from the culture medium by adding 80% (w/v) trichloroacetic acid (150 mL/L) and subsequent centrifugation at 10,000*g* for 10 min. After discarding the pellet, the EPS in the supernatant was precipitated with 3 vol in abs EtOH overnight at −18 °C, and collected by centrifugation at 10,000*g* for 10 min. A soln of the pellet in 40 mL hot distilled water (90 °C) was extensively dialyzed for 72 h against distilled water at 4 °C, then lyophilized. The freeze-dried sample was redissolved in 50 mM sodium phosphate buffer, pH 6.0, and an aliquot (1 mL; 3–10 mg of carbohydrate) was applied to a C16/20 column (Pharmacia Biotech, Uppsala, Sweden), packed with the weakly basic anion exchanger DEAE-Trisacryl Plus M (Sigma Aldrich Chemie GmbH, Taufkirchen, Germany). The neutral EPS was eluted with 50 mM sodium phosphate buffer, pH 6.0 (40 mL), at a flow rate of 0.5 mL/min, monitored at 280 nm with a UV-1 detector (Pharmacia Fine Chemicals, Uppsala, Sweden). The fractions containing the neutral EPS were pooled, desalted by dialysis against distilled water for 48 h at 4 °C, and lyophilized.

3.2. Molecular mass determination

The average molecular mass of the EPS was determined by gel filtration chromatography on a Sephacryl S-400 HR C16/100 column (Amersham Pharmacia Biotech, Uppsala, Sweden), calibrated with dextran standards (M_w 1800, 750, 410, 150, 50, and 25 kDa; Fluka Chemie GmbH, Buchs, Switzerland), using 50 mM phosphate buffer, pH 6.0, containing 150 mM NaCl as eluent. The flow rate was 0.2 mL/min and the fraction size 2 mL. The carbohydrate content of each fraction was determined by the phenol–sulfuric acid assay.[21]

3.3. Monosaccharide analysis

Oligo/polysaccharide was subjected to methanolysis (methanolic 1 M HCl; 18 h, 85 °C). The resulting mixtures of methyl glycosides were trimethylsilylated (1:1:5 hexamethyldisilazane–trimethylchlorosilane–pyridine; 30 min, room temperature), then quantitatively analyzed by GLC as described.[22] In addition, the absolute configurations of the monosaccharides were determined by GLC analysis of the trimethylsilylated (−)-2-butyl glycosides.[23,24] For both analyses, the identities of the monosaccharides were confirmed by gas–liquid chromatography/mass spectrometry (GLC–MS).[22]

3.4. Methylation analysis

Samples (native EPS or oligosaccharide) were permethylated using methyl iodide and solid sodium hydroxide in dimethyl sulfoxide as described previously.[25] For the work-up two protocols were followed. On one hand, the permethylated material was methanolyzed and analyzed as trimethylsilylated methyl glycosides by GLC–MS (monosaccharide analysis protocol, see Section 3.3). On the other hand, the permethylated material was hydrolyzed with 2 M TFA (2 h, 120 °C), and the partially methylated monosaccharides obtained were reduced with $NaBD_4$. Conventional work-up, comprising neutralization and removal of boric acid by co-evaporation with MeOH, followed by acetylation with 1:1 pyridine–Ac_2O (30 min, 120 °C) yielded mixtures of partially methylated alditol acetates, which were analyzed by GLC–MS.[22]

3.5. Gas–liquid chromatography and mass spectrometry

Quantitative GLC analyses were performed on a Chrompack CP9002 gas chromatograph, equipped with an EC-1 column (30 m × 0.32 mm, Alltech, Deerfield, IL) using a temperature program of 140–240 °C at 4 °C/min and flame-ionization detection. GLC–MS analyses were carried out on a GC8060/MD800 system (Fisons instruments, Interscience; 70 eV), using an AT-1 column (30 m × 0.25 mm, Alltech) at the same temperature program.[22]

Matrix-assisted laser desorption ionization time-of-flight mass spectrometry (MALDI-TOF-MS) experiments were performed using a Voyager-DE PRO mass spectrometer (Applied Biosystems, Foster City, CA) equipped with a nitrogen laser (337 nm, 3 ns pulse width). Positive-ion mode spectra were recorded using the reflectron mode and delayed extraction (100 ns). The accelerating voltage was 20 kV with a grid voltage of 75.2%; the mirror voltage ratio was 1.12, and the acquisition mass range 500–3000 Da. Samples were prepared by mixing on the target 1 μL oligosaccharide soln with 1 μL of 2,5-dihydroxybenzoic acid (10 mg/mL) in 50% aqueous acetonitrile as matrix soln.

3.6. Periodate oxidation

To a soln of polysaccharide (30 mg) in 0.1 M NaOAc buffer (35 mL; pH 3.9), $NaIO_4$ was added to a final concentration of 50 mM, and the mixture was kept in the dark for 5 days at 4 °C. Excess of periodate was destroyed by the addition of ethylene glycol (2 mL) after which the soln was dialyzed against tap water. Then, the oxidized polysaccharide was reduced with $NaBH_4$ (2 h; 20 °C), neutralized with 4 M HOAc, dialyzed

against tap water, and lyophilized. The obtained material was subsequently hydrolyzed (0.5 M TFA; 30 min, 80 °C), and the progress of the hydrolysis was monitored by TLC (Merck Kieselgel 60 F254 sheets; 2:1:1 *n*-butanol–acetic acid–water; orcinol/sulfuric acid staining). After concentration, the residue was fractionated on a Bio-Gel P-2 column (60 × 1.5 cm), eluted with 10 mM NH_4HCO_3 at a flow rate of 3 mL/min at room temperature, while monitored by differential refraction index detection. The sugar-containing fraction was lyophilized. A part of the material was directly used for structural analysis. The other part was reduced with $NaBH_4$ (2 h; 20 °C), neutralized with 4 M HOAc, and purified by Bio-Gel P-2.

3.7. NMR spectroscopy

Resolution-enhanced 1D/2D 500-MHz NMR spectra were recorded in D_2O on a Bruker DRX-500 spectrometer (Bijvoet Center, Department of NMR Spectroscopy) at a probe temperature of 27 °C for oligosaccharides and 78 °C for the polysaccharide. Prior to analysis, samples were exchanged twice in D_2O (99.9 at % D, Cambridge Isotope Laboratories, Inc., Andover, MA) with intermediate lyophilization, and then dissolved in 0.6 mL D_2O. Chemical shifts are expressed in parts per million by reference to internal acetone (δ 2.225) for ^1H and/or to the α-anomeric signal of external [1-^{13}C]glucose ($\delta_{C\text{-}1}$ 92.9) for ^{13}C. Suppression of the HOD signal was achieved by applying a WEFT pulse sequence for 1D experiments[26] and by a pre-saturation of 1 s during the relaxation delay for 2D experiments.[27] 2D TOCSY spectra were recorded using an MLEV-17 mixing sequence[28] with spin-lock times of 40–100 ms. 2D ROESY experiments were performed at a mixing time of 300 ms for the oligosaccharide; 2D NOESY experiments were performed with a mixing time of 150 ms for the polysaccharide. Natural abundance 2D ^1H–^{13}C HSQC and HMBC experiments were recorded with and without decoupling, respectively, during acquisition of the ^1H FID. Resolution enhancement of the spectra was performed by a Lorentzian-to-Gaussian transformation or by multiplication with a squared-bell function phase shifted by $\pi/(2.3)$ for 2D spectra, and when necessary, a fifth order polynomial baseline correction was performed. All NMR data were processed using in-house developed software (J. A. van Kuik, Bijvoet Center, Utrecht University).

Acknowledgment

The authors thank Dr. Bas R. Leeflang for assistance with the use of the NMR spectrometer.

References

1. De Vuyst, L.; Degeest, B. *FEMS Microbiol. Rev.* **1999**, *23*, 153–177.
2. Laws, A. P.; Gu, Y.; Marshall, V. M. *Biotechnol. Adv.* **2001**, *19*, 597–625.
3. Uemura, J.; Itoh, T.; Kaneko, T.; Noda, K. *Milchwissenschaft* **1998**, *53*, 443–446.
4. Grobben, G. J.; Smith, M. R.; Sikkema, J.; de Bont, J. A. M. *Appl. Microbiol. Biotechnol.* **1996**, *46*, 279–284.
5. Faber, E. J.; Kamerling, J. P.; Vliegenthart, J. F. G. *Carbohydr. Res.* **2001**, *331*, 183–194.
6. Harding, L. P.; Marshall, V. M.; Hernandez, Y.; Gu, Y.; Maqsood, M.; McLay, N.; Laws, A. P. *Carbohydr. Res.* **2005**, *340*, 1107–1111.
7. Cerning, J.; Bouillanne, C.; Desmazeaud, M. J.; Landon, M. *Biotechnol. Lett.* **1986**, *8*, 625–628.
8. Grobben, G. J.; Sikkema, J.; Smith, M. R.; de Bont, J. A. M. *J. Appl. Bacteriol.* **1995**, *79*, 103–107.
9. Gruter, M.; Leeflang, B. R.; Kuiper, J.; Kamerling, J. P.; Vliegenthart, J. F. G. *Carbohydr. Res.* **1993**, *239*, 209–226.
10. Harding, L. P.; Marshall, V. M.; Elvin, M.; Gu, Y.; Laws, A. P. *Carbohydr. Res.* **2003**, *338*, 61–67.
11. Chaplin, M. F.; Kennedy, J. F. *Carbohydrate Analysis, a Practical Approach*; IRL Press: Oxford, 1986, pp 71–75 and references cited therein.
12. Faber, E. J.; van den Haak, M. J.; Kamerling, J. P.; Vliegenthart, J. F. G. *Carbohydr. Res.* **2001**, *331*, 173–182.
13. Bock, K.; Pedersen, C. *J. Chem. Soc., Perkin Trans. 2* **1974**, 293–297.
14. Bock, K.; Pedersen, C. *Adv. Carbohydr. Chem. Biochem.* **1983**, *41*, 27–66.
15. Faber, E. J.; Zoon, P.; Kamerling, J. P.; Vliegenthart, J. F. G. *Carbohydr. Res.* **1998**, *310*, 269–276.
16. Van Casteren, W. H. M.; Dijkema, C.; Schols, H. A.; Beldman, G.; Voragen, A. G. J. *Carbohydr. Res.* **2000**, *324*, 170–181.
17. Bock, K.; Thøgersen, H. *Annu. Rep. NMR Spectrosc.* **1982**, *13*, 1–57.
18. Bubb, W. A.; Urashima, T.; Fujiwara, R.; Shinnai, T.; Ariga, H. *Carbohydr. Res.* **1997**, *301*, 41–50.
19. Lemoine, J.; Chirat, F.; Wieruszeski, J.-M.; Strecker, G.; Favre, N.; Neeser, J.-R. *Appl. Environ. Microbiol.* **1997**, *63*, 3512–3518.
20. Low, D.; Ahlgren, J. A.; Horne, D.; McManon, D. J.; Oberg, C. J.; Broadbent, J. R. *Appl. Environm. Microbiol.* **1998**, *64*, 2147–2151.
21. Dubois, M.; Gilles, K. A.; Hamilton, J. K.; Rebers, P. A.; Smith, F. *Anal. Chem.* **1956**, *28*, 350–356.
22. Kamerling, J. P.; Vliegenthart, J. F. G. Carbohydrates. In *Mass Spectrometry*; Lawson, A. M., Ed.; Clinical Biochemistry—Principles, Methods, Applications; Walter de Gruyter: Berlin, 1989; Vol. 1, pp 175–263.
23. Gerwig, G. J.; Kamerling, J. P.; Vliegenthart, J. F. G. *Carbohydr Res.* **1978**, *62*, 349–357.
24. Gerwig, G. J.; Kamerling, J. P.; Vliegenthart, J. F. G. *Carbohydr. Res.* **1979**, *77*, 1–7.
25. Ciucanu, I.; Kerek, F. *Carbohydr. Res.* **1984**, *131*, 209–217.
26. Hård, K.; van Zadelhoff, G.; Moonen, P.; Kamerling, J. P.; Vliegenthart, J. F. G. *Eur. J. Biochem.* **1992**, *209*, 895–915.
27. Hård, K.; Vliegenthart, J. F. G. Nuclear Magnetic Resonance Spectroscopy of Glycoprotein-Derived Carbohydrate Chains. In *Glycobiology, a Practical Approach*; Fukuda, M., Kobata, A., Eds.; Oxford University Press: Oxford, 1993; pp 223–242.
28. Bax, A.; Davies, D. G. *J. Magn. Reson.* **1985**, *65*, 355–360.